

Electromagnetic response of high- T_c superconductors

D. Walker and K. Scharnberg

*Abteilung für Theoretische Festkörperphysik, Fachbereich Physik der Universität Hamburg,
Jungiusstrasse 11, D-2000 Hamburg 36, West Germany*

(Received 11 September 1989; revised manuscript received 28 February 1990)

The effective-medium approach is used to calculate the penetration depth, surface resistance, and infrared reflectivity of materials consisting of uniaxial grains embedded in an isotropic background. The grains are taken to be superconducting in the ab plane. The mean-free-path dependence of the ac conductivity in the superconducting state is explicitly taken into account. In the c direction the grains are assumed to be either insulating or poorly conducting. The background is either insulating or normal conducting. In the normal state, all conductivities reduce to Drude expressions. This model should present a reasonable description of high- T_c materials. We predict an increase in the penetration depth by a temperature-independent scale factor. The microwave surface resistance can be fitted, if the samples contain 10–20% of a background material that is a good conductor. This assumption would also explain the less than perfect reflectivity below the absorption edge. If the background is a dielectric, then the absorption edge appears to be shifted to lower frequencies due to void resonances. The shift of this apparent absorption edge with temperature is less than predicted by BCS theory. There seems to be no way to explain large energy gaps sometimes observed in reflectivity by invoking granularity.

I. INTRODUCTION

The electromagnetic response of high- T_c superconductors is not readily explained in terms of the conventional BCS theory. The difficulties are most notable in the temperature dependence of the surface resistance R when plotted versus $1/T$. While BCS theory predicts a rapid fall, followed by an exponential decrease, an almost temperature-independent residual resistance, several orders of magnitude larger than that of Nb or Nb₃Sn, is observed after an initial drop which is fairly sharp but much smaller than expected.^{1–12} Generalizing the BCS theory in order to allow for highly anisotropic energy gaps with nodes on the Fermi surface, does not improve agreement between theory and experiment.¹³

The pronounced dependence of the surface resistance on the *preparation technique* of polycrystalline samples,^{2,4} together with the observation that the residual resistance of epitaxially grown thin films^{1–3,5} or good single crystals¹⁴ can be more than an order of magnitude smaller than that of ceramic material,^{1,7} indicate that the large residual surface resistance is not an intrinsic property of high- T_c superconductors. The most likely sources of the residual losses are inhomogeneities, such as normal or weakly superconducting inclusions, grain boundaries, etc. that one can expect to find in these materials, especially close to the surface. It may seem somewhat surprising then that for frequencies less than about 10 GHz R depends quadratically on frequency^{3,4,11} as predicted by the BCS theory.

The frequency dependence of the far-infrared reflectivity $\mathcal{R}(\omega, T)$ also poses some questions. In most experiments $\mathcal{R}(\omega, T)$ is observed to drop well below 100% even for $T \ll T_c$ long before the absorption edge at $\omega = 2\Delta$ is reached. As in the case of the residual surface

resistance the most plausible explanation for this deviation from the predictions of BCS theory is the assumption that part of the material remains normal conducting,^{15–17} although in this case an anisotropic gap with nodes would give similar results.¹³

In addition to the ubiquitous structural and compositional defects there is the pronounced normal-state anisotropy which further aggravates the problem of interpreting the experimental data. Whether inhomogeneity and anisotropy are responsible for the fact that energy gaps 2Δ deduced from reflectivity data range from $\sim 2.5T_c$ to $\sim 8T_c$ at zero temperature^{16–25} and show much weaker temperature dependences than predicted by BCS theory,^{17,26,27} is a question that will be addressed and partially resolved in this paper.

A general framework within which to obtain the electromagnetic response of inhomogeneous and anisotropic superconductors is provided by the *effective-medium approach* (EMA).^{15,28–30} It can be derived from the coherent-potential approximation³¹ and thus has a very sound theoretical foundation.

Within the EMA an inhomogeneous material is described as a mixture of several types of ellipsoidal grains, each type endowed with its dielectric tensor. Calculating the dielectric tensor of the effective medium involves an average with respect to grain orientations. For randomly oriented grains the effective medium turns out to be isotropic.³⁰

The EMA can be used only if the grain size d is much less than the wavelength λ of the incident radiation. In the microwave regime, the inequality $d \ll \lambda$ is easily fulfilled, but it begins to break down in the infrared regime at frequencies above but close to the BCS energy gap $2\Delta = 3.5T_c$. Some authors^{32,33} have, therefore, preferred to compare the experimental results to an averaged

reflectivity, rather than the reflectivity of an averaged, i.e., effective medium. Doll *et al.*³⁴ compare both approaches.^{32,13} Because of this problem with the EMA in the high-frequency regime we have made no attempt to generalize the model sufficiently to describe features of the ir reflectivity at frequencies well above the expected gap.²²⁻²⁵

The EMA implicitly assumes strong couplings between grains. It can be argued that at least in the sintered ceramics the superconducting grains are only weakly coupled through Josephson tunneling.³⁵⁻³⁸ The dependence of the Josephson coupling on magnetic field is likely to contribute to the complex behavior of microwave absorption in a magnetic field, and it could also lead to a nonlinear response.^{36,37} Depending on the quality of the samples, such nonlinear response can be observed.^{2,14} In the absence of applied magnetic fields and at low power levels of the electromagnetic radiation the question of coupling strength seems to be largely irrelevant, and we believe that the results presented here should adequately describe several sets of experiments. The effective-medium approach has been applied previously to the infrared reflectivity of superconductors with the assumptions that the samples were either homogeneous but anisotropic,^{19,20,34} or isotropic but consisting of two different components.^{16,17,15}

In order to develop a more realistic picture of a sintered superconducting ceramic, we consider a *two-component* material, consisting of electrically uniaxial grains which are superconducting in the *ab* plane and insulating or normal conducting along the *c* axis, dispersed on an isotropic background material. As a background, we have considered a dielectric, corresponding to a spongelike sample where the inclusions are air in the simplest case, and, alternatively, a Drude conductor, assuming that parts of the sample remain normal conducting below T_c .

II. GENERAL THEORY

A. Effective-medium approach

In order to describe a two-component medium, one regards individual grains of ellipsoidal shape from either type of material as being embedded in a homogeneous effective medium that is supposed to possess the average electrical properties sought for.^{15,28,29} If the grain is from the first medium, say *a*, which we assume to be anisotropic, it is penetrated by a field given by^{28,39}

$$\mathbf{E}_a^{(n)} = \sum_{i=1}^3 \frac{\epsilon_{\text{EMA}}}{(1-g_i)\epsilon_{\text{EMA}} + g_i\epsilon_i^{(a)}} \hat{\mathbf{a}}_i^{(n)} \hat{\mathbf{a}}_i^{(n)\text{T}} \mathbf{E}_{\text{eff}}, \quad n=1,2,\dots,N_a. \quad (1)$$

$(\hat{\mathbf{a}}_1^{(n)}, \hat{\mathbf{a}}_2^{(n)}, \hat{\mathbf{a}}_3^{(n)})$ is the set of unit vectors along the dielectric principal axes of the *n*th grain ($n=1,2,\dots,N_a$), and the superscript **T** denotes the transpose of (column) vectors. The geometric shape of each grain has been taken to agree with its dielectric anisotropy so that the dielectric and the depolarization tensors can be diagonalized

simultaneously with eigenvalues $(\epsilon_1^{(a)}, \epsilon_2^{(a)}, \epsilon_3^{(a)})$ and (g_1, g_2, g_3) , respectively.

Equation (1) is valid only if the effective medium is isotropic. For this to be the case, the anisotropic grains have to be randomly oriented. This precludes a quantitative discussion of polycrystalline films with preferred orientation of crystallites, except in the special case that all grains are aligned.

The grains of the second medium, called *b*, are treated in the same manner, since the EMA considers both media symmetrically. In the present case, medium *b* is taken to be an isotropic background originating, for example, from highly disordered intergrain material. We thus expect no orientation effects, so that it seems adequate to consider spherical grains only. Then $g_1=g_2=g_3=\frac{1}{3}$, and the field that penetrates one of these grains is simply given by^{28,39}

$$\mathbf{E}_b^{(n)} = \frac{3\epsilon_{\text{EMA}}}{2\epsilon_{\text{EMA}} + \epsilon_b} \mathbf{E}_{\text{eff}}. \quad (2)$$

To acquire self-consistency, the effective field is taken to be the algebraic average of the internal fields of the particular grains:²⁸

$$\mathbf{E}_{\text{eff}} = f \frac{1}{N_a} \sum_{n=1}^{N_a} \mathbf{E}_a^{(n)} + (1-f) \frac{1}{N_b} \sum_{n=1}^{N_b} \mathbf{E}_b^{(n)}. \quad (3)$$

f denotes the volume fraction occupied by the medium *a*. From this, the self-consistency equation in dyadic form is obtained by inserting $\mathbf{E}_{a,b}^{(n)}$ from (1) and (2):²⁸

$$\mathbf{E}_{\text{eff}} = f \sum_{i=1}^3 \frac{\epsilon_{\text{EMA}}}{(1-g_i)\epsilon_{\text{EMA}} + g_i\epsilon_i^{(a)}} \frac{1}{N_a} \sum_{n=1}^{N_a} \hat{\mathbf{a}}_i^{(n)} \hat{\mathbf{a}}_i^{(n)\text{T}} \mathbf{E}_{\text{eff}} + (1-f) \frac{3\epsilon_{\text{EMA}}}{2\epsilon_{\text{EMA}} + \epsilon_b} \mathbf{E}_{\text{eff}}. \quad (4)$$

Since we have used a scalar permittivity for the effective medium, a random orientation of the N_a anisotropic grains must be assumed. It is then feasible to replace the sum over the crystallites by an integral over Euler angles.²⁸ This approximation renders the dyads in (4) diagonal:

$$\frac{1}{N_a} \sum_{n=1}^{N_a} \hat{\mathbf{a}}_i^{(n)} \hat{\mathbf{a}}_i^{(n)\text{T}} \approx \frac{1}{3} \mathbf{1}, \quad i=1,2,3,$$

and thus leads to a single equation for ϵ_{EMA} . For simplicity we consider only systems with uniaxial symmetry and are thus forced to ignore the slight orthorhombic distortion in superconducting $\text{Y}_1\text{Ba}_2\text{Cu}_3\text{O}_{7-\delta}$. Then the eigenvalues of the dielectric tensor are $\epsilon_1^{(a)}=\epsilon_2^{(a)}=\epsilon_{\perp}$ and $\epsilon_3^{(a)}=\epsilon_{\parallel}$. For the sake of consistency, the uniaxial grains are assumed to be spheroids. Then $2g_{\perp}=1-g_{\parallel}$ because the trace of the depolarization tensor is 1. With these simplifications and assumptions we arrive at the following self-consistency equation:²⁸

$$f \left[2 \frac{(1-g_{\parallel})(\epsilon_{\text{EMA}} - \epsilon_{\perp})}{(1+g_{\parallel})\epsilon_{\text{EMA}} + (1-g_{\parallel})\epsilon_{\perp}} + \frac{g_{\parallel}(\epsilon_{\text{EMA}} - \epsilon_{\parallel})}{(1-g_{\parallel})\epsilon_{\text{EMA}} + g_{\parallel}\epsilon_{\parallel}} \right] + 3(1-f) \frac{\epsilon_{\text{EMA}} - \epsilon_b}{2\epsilon_{\text{EMA}} + \epsilon_b} = 0. \quad (5)$$

From this, we obtain a third-order polynomial in ϵ_{EMA} that can easily be solved. The physical solution is the one that has a *positive imaginary part* ϵ''_{EMA} .

As in the case of a one-component uniaxially anisotropic EMA, which has been shown by Stroud³⁰ to be identical to a two-component isotropic EMA with $f = \frac{2}{3}$, the present theory is identical to a three-component isotropic EMA with $f_{\perp} = \frac{2}{3}f$, $f_{\parallel} = \frac{1}{3}f$ and $f_b = 1 - f$. For $f = \frac{3}{4}$ the background (ϵ_b) and the c direction (ϵ_{\parallel}) can be interchanged without affecting ϵ_{EMA} .

If $f = 1$ there is no background medium, and (5) reduces to a quadratic equation in ϵ_{EMA} , which describes an anisotropic medium.²⁸ Only Noh *et al.*²⁰ and Sulewski *et al.*¹⁹ have used such an equation studying specifically the effects of nonspherical grain shapes. Their equation, however, differs significantly from our (5) with $f = 1$ if $g_{\parallel} \neq \frac{1}{3}$. Due to factors involving g_{\parallel} , which are missing in the numerator, they do not find a metal-insulator transition for platelike grains insulating in the c direction (see Sec. III).

The equation for the effective dielectric function used by Noh *et al.*²⁰ and Sulewski *et al.*¹⁹ has first been derived by Stroud,³⁰ who defines an effective conductivity through $\langle \mathbf{J} \rangle = \vec{\sigma}_e \langle \mathbf{E} \rangle$ [Ref. 30, Eq. (2.1)]. Unfortunately, contrary to the statement following this equation, the average field $\langle \mathbf{E} \rangle$ differs from the relevant electric field, designated \mathbf{E}_0 in Stroud's paper, by a finite depolarization field (Ref. 39, footnote on p. 44) if the grains are nonspherical. Our Eq. (5) has been designed to ensure that this depolarization field vanishes. It is obvious from the derivation of (5) given here, that no discrepancy between the two approaches will arise when no average with respect to grain orientation is required as, for example, in the problem studied by Garner and Stroud.¹⁵

B. Electrodynamics

Once the dielectric function ϵ_{EMA} of the effective medium has been obtained, several measurable quantities can be derived. Since the high- T_c superconductors are extreme type II, it is possible to treat the electrodynamics in the *local limit*, which simplifies the calculations considerably.¹³

In order to compare the EMA theory with experimental curves, we examine the behavior of the *reflectivity*, the *surface resistance*, and the *penetration depth*. In the local limit, these quantities are obtained from the following for-

mulas:^{13,39,40} Reflectivity:

$$\mathcal{R} = \left| \frac{\sqrt{\epsilon_{\text{EMA}} - 1}}{\sqrt{\epsilon_{\text{EMA}} + 1}} \right|^2, \quad (6a)$$

Surface resistance:

$$R = \frac{4\pi}{c} \text{Re} \frac{1}{\sqrt{\epsilon_{\text{EMA}}}}, \quad (6b)$$

Penetration depth:

$$\lambda = \lim_{\omega \rightarrow 0 \text{Im}} \frac{c}{(\omega^2 \epsilon_{\text{EMA}})^{1/2}}. \quad (6c)$$

Note that these expressions are derived under the assumption that the material fills a half-space. They are, therefore, not applicable to thin-film experiments when the penetration depth exceeds the film thickness.

C. Choice of dielectric functions

The relations (6) hold, whatever dielectric function may be inserted. To account for the suggested two-dimensionality of $\text{YBa}_2\text{Cu}_3\text{O}_{7-\delta}$, we assume that the crystallites are superconducting in the ab plane and insulating or Drude-conducting along the c axis. So the eigenvalues of the dielectric tensor in Eq. (5) are chosen as

$$\epsilon_{\perp} = \epsilon_{\text{BCS}} \text{ OR } \epsilon_{\text{unconventional}},$$

$$\epsilon_{\parallel} = \text{const OR Drude}.$$

We concentrate on the simplest kind of superconducting state because there is no compelling evidence for unconventional pairing. The penetration depth, for example, appears to have the temperature dependence expected of conventional superconductors,^{41,42} although there is still some controversy.⁹ Because of this ongoing discussion we have also used expressions for ϵ_{\perp} (and ϵ_{\parallel}) appropriate for the polar state and the Anderson-Brinkman-Movel (ABM) state¹³ wherever it seemed conceivable that nodes in the energy gap might offer an easy explanation for the experimental observations.

The transverse BCS dielectric function has been calculated within the framework of a linear response theory, via the current-current correlation function:^{13,43}

$$\epsilon_{\text{BCS}}(\mathbf{q}, \omega) = 1 - \frac{\omega_p^2}{\omega^2} \left[1 + \frac{m}{n} \langle [j_x, j_x] \rangle(\mathbf{q}, \omega) \right]. \quad (7)$$

Here, $\omega_p = (4\pi e^2 n / m)^{1/2}$ is the plasma frequency.

Since the electrodynamics is local, only the limit $\mathbf{q} \rightarrow 0$ needs to be considered. In order to obtain $\epsilon_{\text{BCS}}(\omega)$ one then has to evaluate the integral:^{13,43}

$$\begin{aligned} 1 + \frac{m}{n} \langle [j_x, j_x] \rangle(0, \omega) &= \text{Re} \int_{\Delta - \omega}^{\Delta} d\Omega \tanh \frac{\Omega + \omega}{2T} \frac{1}{E_2 - \bar{E}_1 + 2i\Gamma} \left[1 + \frac{(\Omega + \omega)\Omega + \Delta^2}{E_2 \bar{E}_1} \right] \\ &+ \frac{1}{2} \int_{\Delta}^{\infty} d\Omega \left[\tanh \frac{\Omega + \omega}{2T} - \tanh \frac{\Omega}{2T} \right] \left[1 + \frac{(\Omega + \omega)\Omega + \Delta^2}{E_2 E_1} \right] \frac{1}{E_2 - E_1 + 2i\Gamma} \\ &+ \frac{1}{2} \int_{\Delta}^{\infty} d\Omega \left[\frac{\tanh(\Omega/2T)}{E_2 + E_1 + 2i\Gamma} + \frac{\tanh[(\Omega + \omega)/2T]}{E_2 + E_1 - 2i\Gamma} \right] \left[1 - \frac{(\Omega + \omega)\Omega + \Delta^2}{E_2 E_1} \right]. \end{aligned}$$

$$\begin{aligned} E_1 &= (\Omega^2 - \Delta^2)^{1/2}, \\ \bar{E}_1 &= -i(\Delta^2 - \Omega^2)^{1/2}, \\ E_2 &= [(\Omega + \omega)^2 - \Delta^2]. \end{aligned} \quad (8)$$

In view of the fact that high- T_c materials are intrinsically clean ($l > \xi_0$) we have kept the normal-state scattering rate

$$\Gamma = \frac{1}{2\tau} = 0.88 \frac{\xi_0}{l} \pi T_c \quad (9)$$

arbitrary. The Mattis-Bardeen result⁴⁴ follows from (8) in the limit $\Gamma \rightarrow \infty$.

III. RESULTS AND DISCUSSION

For very low frequencies, an analytical result can be obtained for ϵ_{EMA} by retaining in (5) only the most divergent quantity $\epsilon'_1 = \text{Re}\epsilon_{\text{BCS}} \propto \omega^{-2}$. If the effective medium is to be a superconductor, ϵ_{EMA} must show the same low-frequency behavior. This leads to

$$\lim_{\omega \rightarrow 0} \omega^2 \epsilon_{\text{EMA}} = \frac{a_\perp}{a_0} \lim_{\omega \rightarrow 0} \omega^2 \epsilon_1, \quad (10)$$

with

$$a_\perp = f(7 - 9g_\parallel) - 3(1 - g_\parallel)$$

and

$$a_0 = f \frac{(1 - 3g_\parallel)^2}{1 - g_\parallel} + 3(1 + g_\parallel).$$

If the grains are also superconducting along the c axis but with $\epsilon_\parallel \neq \epsilon_\perp$, as is the case for unconventional superconducting states (e.g., polar state, ABM state¹³), then (5) reduces only to a quadratic equation for ϵ_{EMA} in the limit $\omega \rightarrow 0$, yielding a more complicated result than (10).

The effective medium ceases to be a superconductor when the numerator a_\perp in (10) vanishes. Thus we find a critical volume fraction

$$f_c = \frac{3(1 - g_\parallel)}{7 - 9g_\parallel} \quad (11)$$

of the superconducting material at which the effective medium undergoes a transition from the superconducting to the normal conducting or insulating state.

For spherical grains ($g_\parallel = \frac{1}{3}$), f_c reduces to $\frac{1}{2}$ as expected for a two-dimensional (2D) medium. It is interesting to note, however, that f_c depends on the grain shape, increasing from a minimum value $f_c = \frac{3}{7}$ for extremely prolate spheroids ($g_\parallel = 0$). Since f_c cannot exceed 1, a critical value $g_\parallel^c = \frac{2}{3}$, corresponding to an aspect ratio of 3.408, exists above which a medium consisting purely of

randomly oriented anisotropic platelike superconducting grains becomes insulating or normal conducting.

We feel that this dependence of the transition on the grain shape is very plausible: For the platelets considered here, currents can pass only through a small fraction of their surfaces close to the equatorial planes. If such platelets are randomly oriented, it seems clear that, as g_\parallel is increased, it becomes more difficult and eventually impossible to find a continuous (super)conducting path through the sample.

Since the effective-medium approach is a mean-field approximation, the behavior of the dielectric function in the vicinity of the transition is not accurately described by the EMA,¹⁵ nor can we expect the dependence of f_c on g_\parallel determined previously to be quantitatively correct. We do believe, however, that (11) does at least qualitatively reflect an important physical trend.

Because of these limitations of the EMA we would like to emphasize that we are not interested in the details of the superconductor-insulator or normal conductor transition. Instead, we want to use the EMA to describe disordered anisotropic materials well above this transition in order to offer explanations for experimentally observed deviations from the BCS theory.

A. Penetration depth

It follows from (6c) and (10) that the only way in which granularity changes the penetration depth of a uniaxial superconductor that is superconducting only in the basal plane, is to increase it by a temperature-independent scale factor:

$$\lambda_{\text{EMA}} = \sqrt{a_0/a_\perp} \lambda_\perp.$$

One can, therefore, expect a marked dependence of the zero-temperature penetration depth $\lambda(0)$ on preparation techniques without a concomitant change in the temperature dependence of the penetration depth. This is indeed observed.⁴² Unfortunately, since absolute measurements of $\lambda(0)$ are not very reliable,⁴¹ experiments do not provide a stringent test for this theory and, in particular, do not allow any inference on the parameters (f , g_\parallel , ϵ_b , etc.) involved. Note that, while λ_\perp depends through (8) on the scattering rate Γ (9) and thus on the normal-state dc conductivity

$$\sigma_{0\perp} = \omega_{p\perp}^2 / 8\pi\Gamma_\perp \quad (12)$$

of the CuO_2 planes, there is no simple relationship between λ_{EMA} and the normal-state dc conductivity of the macroscopic effective medium, which is easily obtained from (5) if $\epsilon_\parallel = \text{const}$ is assumed:

$$\sigma_{\text{EMA}} = \frac{1}{2a_0} (a_\perp \sigma_{0\perp} - a_b \sigma_{0b}) + \frac{1}{2a_0} [(a_\perp \sigma_{0\perp} + a_b \sigma_{0b})^2 + 36f(1-f)(1-g_\parallel)\sigma_{0b}\sigma_{0\perp}]^{1/2}. \quad (13)$$

Here we have introduced the abbreviation

$$a_b = f(5 - 3g_{\parallel}) / (1 - g_{\parallel}) - 3(1 + g_{\parallel}).$$

It seems that experimental results are equally compatible with theories based on Josephson coupled grains.^{35,38,45}

B. Surface resistance

To illustrate the scope of the present theory we calculate numerically the temperature and frequency dependence of the surface resistance for a few representative sets of parameter values. No attempt is made to obtain best fits to existing experimental data.

Frequencies, energies, and conductivities are normalized to (πT_c) . To the plasma frequency appearing in (7) we assign a value of $24.15\pi T_c$ which corresponds to 0.62 eV if the transition temperature is 94 K. Similarly low values have been used by other authors.^{18,33} The scattering rates (9) are chosen as $\Gamma = 0.1\pi T_c$ ($\tau = 1/2\Gamma = 1.3 \times 10^{-13}$ sec) and $\Gamma = \pi T_c$ in agreement with the generally

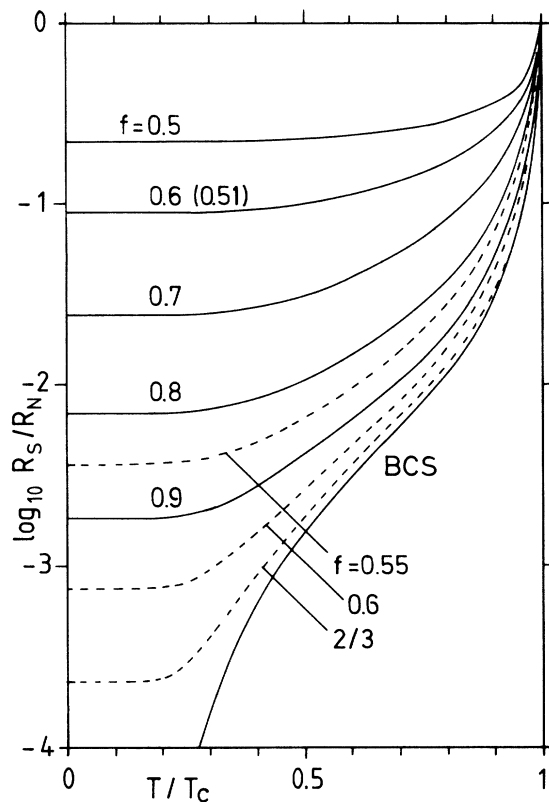


FIG. 1. EMA surface resistance for uniaxial grains of spherical shape, insulating along the c axis, in a Drude conducting background. The logarithm of the ratio of the surface resistances in the superconducting and normal conducting states is plotted versus temperature for various filling fractions f of the superconducting component. The frequency is $\omega = 0.0165\pi T_c$, which corresponds to 100 GHz, if T_c is assumed to be 94 K. The solid curves correspond to a background plasma frequency ω_{pb} of $24.2\pi T_c$ (0.62 eV), the dashed ones to $2.42\pi T_c$. In both cases, $\Gamma_b = \pi T_c$. The normal-state parameter values of the superconducting grains are in both cases $\Gamma_{\perp} = \pi T_c$, $\omega_{p\perp} = 24.2\pi T_c$, $\epsilon_{\parallel} = 4$.

held view that high- T_c materials are intrinsically clean superconductors. These parameter values yield dc conductivities $\sigma_0 = 232\pi T_c [10(\text{m}\Omega \text{ cm})^{-1}]$ and $\sigma_0 = 23.2\pi T_c$ almost spanning the range of observed conductivities.⁸⁻¹⁰

If the background and superconducting grains in the c direction are both described by real and not extravagantly large permittivities, then ϵ_{\perp} is the leading term in (5), since surface resistance measurements are performed at frequencies well below the gap. Hence we still would have $\epsilon_{\text{EMA}} \propto \epsilon_{\perp}$ [Eq. (10)] so that the frequency and temperature dependence of the normalized surface resistance above the percolation threshold should be that of a superconductor, independent of composition and grain shape. To account for the experimental observations it is, therefore, necessary to assume the presence of normal conducting material. In view of the highly anisotropic dc conductivity observed in single crystals we assume that it is the background material that is normal conducting. The superconducting grains are taken to be insulating in the c direction with $\epsilon_{\parallel} = 4$. Introducing a finite conductivity $\sigma_{0\parallel}$ in the c direction by choosing $\omega_{p\parallel} \ll \omega_{p\perp}$ has no effect on our results as long as the conductivity in the background material σ_{0b} is much larger than $\sigma_{0\parallel}$.

Figures 1 and 2 show semilogarithmic plots of the re-

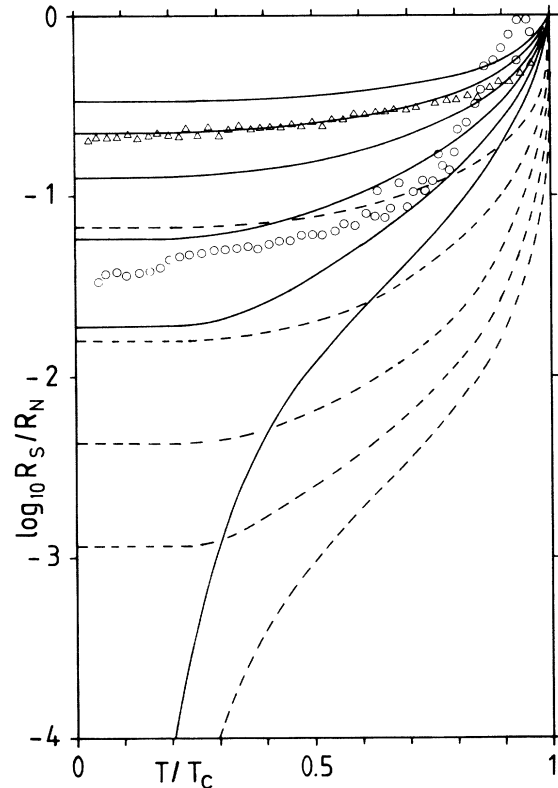


FIG. 2. Same as Fig. 1, except for a tenfold increase in the normal-state dc conductivities $\sigma_{0\perp} = \sigma_{0b}$ [Eq. (12)]. $\Gamma_{\perp} = \Gamma_b = 0.1\pi T_c$, $\omega_{p\perp} = \omega_{pb} = 24.2\pi T_c$ (solid curves); $\Gamma_{\perp} = \Gamma_b = 2.5\pi T_c$, $\omega_{p\perp} = \omega_{pb} = 121\pi T_c$ (dashed curves). Other parameters are the same as in Fig. 1: $\epsilon_{\parallel} = 4$, $\omega = 0.0165\pi T_c$. For each set of curves the residual resistance increases monotonically with decreasing filling fraction f . Curves shown belong to $f = 1.0, 0.9, 0.8, 0.7, 0.6$. For $f = 0.5$, only the full curve has been included. Superimposed are experimental data supplied by Grüner (Refs. 1 and 3).

duced surface resistance versus reduced temperature for one of the highest frequencies studied experimentally,^{1,8,9} i.e., $\omega/2\pi = 102$ GHz, which, for $T_c = 94$ K, corresponds to $\omega = 0.0165\pi T_c$. Grains are taken to be spherical. The full curves present results obtained for various superconducting volume fractions f when the normal-state parameters (ω_p, Γ) of the background material and the superconducting grains are identical.

Since, according to BCS theory, R_s/R_n increases as the superconductor becomes purer, the EMA result for R_s/R_n also increases when the scattering rates for both the superconducting and the normal components are decreased. This is shown in Fig. 2, where the full curves differ from those in Fig. 1 by a reduction in Γ from πT_c to $0.1\pi T_c$.

The dashed curves in Fig. 1 are obtained when the plasma frequency ω_{pb} of the background is reduced by a factor 10 so that $\sigma_{0b} = \sigma_{0l}/100$. In this case, deviations from BCS theory are small except at very low temperatures or very close to the percolation limit. In order to reproduce the large residual resistances observed in ceramics^{1,7} we would have to assume $f \sim 0.5$. This, however, would result in an extremely sensitive dependence of the residual resistance on composition and preparation technique contrary to experimental findings. It seems necessary, therefore, to assume that high- T_c pellets or polycrystalline films contain some *highly conducting* material that remains normal conducting at all temperatures.

According to Fig. 1 we need some 20% of a good normal conductor to account for 1% residual resistance. This seeming discrepancy⁷ arises, of course, from the sharp reduction in the penetration depth. The presence of an even larger fraction of normal metal would have had to be assumed if we had used a higher plasma frequency, because then the London penetration depth $\lambda_L = c/\omega_p$ would have been smaller. This effect can be seen in Fig. 2 where the dashed curves are for a plasma frequency of 3.1 eV.¹⁸ Together with increasing ω_p we have increased Γ in such a way that R_n remained unchanged.

In the case of anisotropic grains considered here, the amount of normal metal required to account for a fixed residual resistance depends on grain shape: Curves practically identical to the full curve in Fig. 1 marked $f = 0.8$ are obtained for $f = 0.9$ when the grains are platelets with $g_{\parallel} = \frac{1}{2}$ (aspect ratio $a/c = 1.82$) and for $f = 0.7$ when the grains are needles with $g_{\parallel} = \frac{1}{30}$ (aspect ratio $a/c = 0.139$). Averaging platelets rather than spheres or needles with respect to orientation of their dielectric axes effectively increases the conductivity of the isotropic normal component relative to that of the superconducting material and thus leads to higher losses. A predominantly a -axis-oriented film would, therefore, show a higher reduced surface resistance R_s/R_n than a c -axis-oriented film, even if the amount and quality of the normal metal present were the same.⁸

Superimposed on our calculated curves in Fig. 2 are experimental data obtained by Awasthi *et al.*¹ on $\text{YBa}_2\text{Cu}_3\text{O}_{7-\delta}$ ceramics (triangles) and films (circles).

There appears to be broad agreement between theory and experiment, with the ceramics requiring a smaller value of f than the film, as expected. It is interesting to note that for the ceramic the transition at T_c is even narrower than predicted by the EMA. Unless much broader transitions are observed² it seems unnecessary, therefore, to generalize the EMA further to take a spread in T_c 's into account.⁷

Agreement between the film data and our calculations is rather poor near T_c . This is most likely due to the normal-state penetration depth exceeding the film thickness which leads to losses in the substrate. This problem is well known in the study of high-quality thin films^{5,8-10} and necessitates special consideration¹⁰ to extract values of R_s/R_n that can be compared with this theory.

At low temperatures, the film results do not seem to saturate as our theory predicts. Such small temperature variation below $T_c/2$ has been observed in several experiments.^{2,8-10} In most cases it can be fitted to a linear T dependence.^{8,9} Even though the slope is sample dependent, it has been speculated that this power law may be due to nodes in the energy gap,⁹ pointing to unconventional pairing.

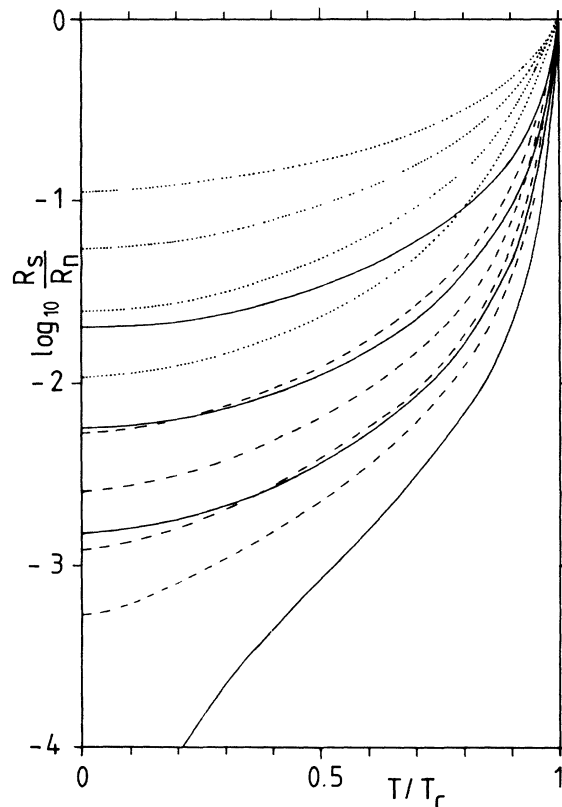


FIG. 3. Reduced surface resistance for a composite medium consisting of a normal metal and an unconventional superconductor with nodes in the energy gap. Dashed curves: $\epsilon_{\perp} = \epsilon_{\perp}^{\text{ABM}}$, $\epsilon_{\parallel} = \epsilon_{\parallel}^{\text{ABM}}$; solid curves: $\epsilon_{\perp} = \epsilon_{\perp}^{\text{ABM}}$, $\epsilon_{\parallel} = 4$; dotted curves: $\epsilon_{\perp} = \epsilon_{\perp}^{\text{pol}}$, $\epsilon_{\parallel} = 4$. Each set of curves consists of results for filling fractions $f = 1.0, 0.9, 0.8, 0.7$. The normal-state parameters are the same as those for the solid curves in Fig. 1: $\omega_{p\perp} = \omega_{p\parallel} = 24.2\pi T_c$, $\Gamma_{\perp} = \Gamma_{\parallel} = \pi T_c$, $\epsilon_{\parallel} = 4$.

In order to investigate the feasibility of this explanation we show in Fig. 3 results for unconventional pair states with nodes on the c axis (ABM state, solid curves and dashed curves) or a line of nodes in the ab plane (polar state, dotted curves). These states do not represent realistic choices for possible unconventional pair states in high T_c superconductors, but they can provide us with an idea about possible consequences of nodes in the energy gap. Parameters are the same as for the solid curves in Fig. 1, only the permittivities ϵ_{\perp} and ϵ_{\parallel} entering (5) are chosen differently. For the dashed curves we have chosen ϵ_{\perp} and ϵ_{\parallel} appropriate for the ABM state.¹³ The EMA then leads to an average over the anisotropic gap. As can be seen from the lowest dashed curve, corresponding to $f=1$, the drop in R_s/R_n between T_c and $0.6T_c$ is practically independent of the details of the superconducting state and merely reflects the decrease in penetration depth, as was pointed out before.¹³ At low temperatures the decrease of R_s/R_n is more gradual than the exponential dependence resulting from an isotropic gap, and one does indeed find a finite surface resistance at $T=0$ (cf. Fig. 11 in Ref. 13). This, however, is much lower than what is observed even in good films so that we again have to invoke the presence of normal conducting material which then dominates $R_s(T)$ at low T .

To take the near-insulating behavior in the c direction into account we have also considered the case $\epsilon_{\perp} = \epsilon_{\perp}^{\text{ABM}}$ and $\epsilon_{\parallel} = 4$. With this choice, the solid curves are obtained. The result for $f=1$ is very low, because in this geometry the current flows in the direction of maximum energy gap. Using $\epsilon_{\perp} = \epsilon_{\perp}^{\text{ABM}}$ in (5) is not feasible because this introduces anisotropy in the basal plane.

In order to obtain a large intrinsic low-temperature surface resistance we have used for ϵ_{\perp} the permittivity $\epsilon_{\perp}^{\text{polar}}$ of a polar state¹³ while keeping $\epsilon_{\parallel} = 4$. This way, the line of nodes makes itself felt most strongly (Fig. 3, dotted curves). Now, the effect of additional losses in a normal component is less significant so that values of $(1-f)$ similar to those of a 2D BCS superconductor are required to fit the data obtained on ceramics.

Such unconventional pair states do, however, predict a stronger variation of R_s/R_n at low temperatures. All curves in Fig. 3 except the full curve corresponding to $f=1$ are, to a very good approximation, parabolas for $T \leq 0.6T_c$. Hence, nodes in the energy gap cannot account for the linear T dependence most frequently observed. Our guess would be that it originates from those inelastic-scattering processes that are responsible for the linear T_c dependence of the normal-state resistivity.

The frequency dependence of R_s has also been the subject of intense study. Due to the sample dependence of R_s at low T one should not expect $R_s(\omega)$ to follow a universal law, but indications were that $R_s(\omega) \propto \omega^2$ in agreement with BCS theory. Recent measurements on one and the same film at widely different frequencies have confirmed this quadratic dependence, although the error bars at $T_c/3$ are considerable.¹¹

This result may seem surprising in view of the fact that the low-temperature surface resistance is determined by losses in a normal conducting fraction. From Fig. 4 it

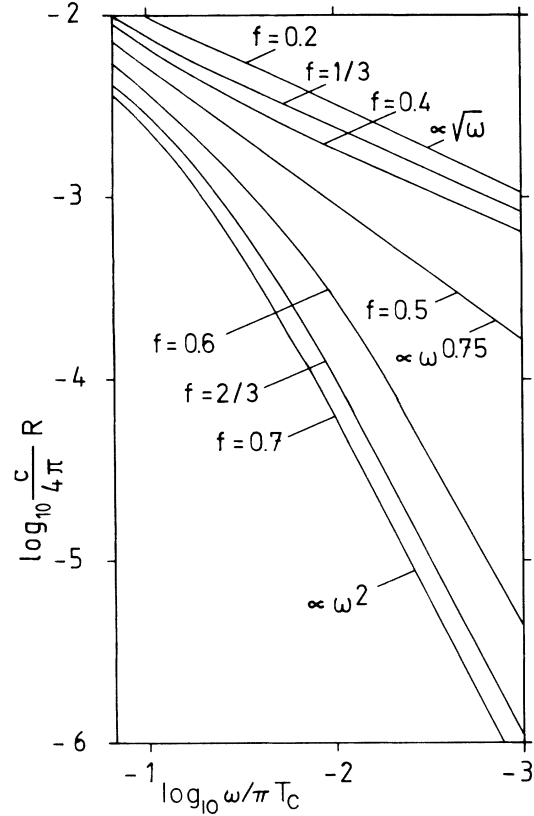


FIG. 4. EMA surface resistance for uniaxial grains, insulating along the c axis, on a Drude conducting background at $T=0.2T_c$ vs frequency, on a double logarithmic scale. With decreasing f , the low-frequency behavior changes from an ω^2 to an $\omega^{1/2}$ progression. $\omega_{p\perp} = \omega_{pb} = 24.2\pi T_c$, $\Gamma_{\perp} = \Gamma_b = \pi T_c$, $\epsilon_{\parallel} = 4$.

can be seen that our EMA calculations give such a quadratic frequency dependence even for a rather large volume fraction $(1-f)$ of the normal conducting material. This frequency dependence of R_s has its origin in the low-frequency divergence of the imaginary part of the conductivity which is a universal feature of the superconducting state. At low frequencies [$\omega \ll \Delta(T)$, $\omega \ll \Gamma$] and low reduced temperatures one can expand (6b) and (6c) to obtain

$$R = \frac{\sqrt{4\pi\omega}}{2c} \frac{\sigma'_{\text{EMA}}}{(\sigma''_{\text{EMA}})^{3/2}} = \frac{4\pi}{c} \omega^2 2\pi \sigma'_{\text{EMA}} \lambda_{\text{EMA}}^3.$$

If the residual losses originate from the normal conducting background, then σ'_{EMA} is simply given by

$$\sigma'_{\text{EMA}} = \frac{36f(1-f)(1-g_{\parallel})}{a_0 a_1} \sigma_{0b}$$

which differs from the conductivity (13) of the composite medium and thus would be difficult to determine independently.

It is only below the percolation limit, when the effective medium is no longer a superconductor, that a

different behavior is observed (Fig. 4). At finite frequencies, the transition from superconductor to normal conductor as a function of f is blurred (Fig. 4).

C. Reflectivity

Numerical results are presented and discussed for anisotropic composite media in order to illustrate the salient features of the present theory, not to fit a few of the many existing data sets. This is our reason for not including the effect of phonons.¹⁹ Previous applications of the effective-medium theory to the infrared reflectivity are extended to include both anisotropy in the superconducting grains and the presence of a normal or insulating component. The conductivity in the superconducting state is calculated for arbitrary mean free paths.

The reflectivity of a polycrystalline sample consisting of uniaxial crystallites embedded in a Drude conducting material is displayed in Fig. 5. Again, the individual grains are supposed to be BCS superconductors in the ab plane and insulating along the c axis with an assumed dielectric constant ϵ_{\parallel} of 4. The impurity scattering rate Γ of the background material is chosen to be greater than that of the grains by a factor of 10 while the plasma frequencies are the same. The curves have been computed for a temperature of $0.5T_c$.

Below the gap frequency 2Δ , the only absorption is that from the excited quasiparticles which, at $T=0.5T_c$, is already negligible. If f is lowered successively, Ohmic losses in the background become more and more dominant, and for $f \rightarrow 0$, $\mathcal{R}(\omega)$ tends towards the Drude curve of a normal metal.

This transition from a superconductor to a normal metal is visible most clearly in the slope of $\mathcal{R}(\omega)$ at $\omega=0$, as shown in the inset of Fig. 5. There are a horizontal tangent and a downward curvature if $f > \frac{1}{2}$. Below, there are no continuous supercurrents through the sample, and

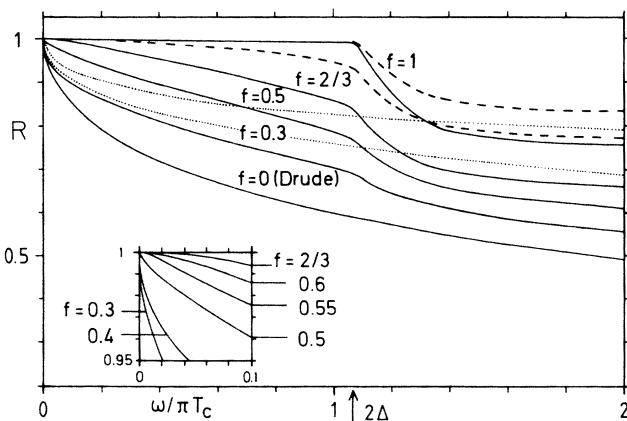


FIG. 5. EMA reflectivity at $T=0.5T_c$ for uniaxial grains, insulating along the c axis, on a Drude conducting background. In the inset, the low-frequency behavior with the change from a horizontal tangent to a Hagen-Rubens-like vertical one at $\omega=0$ is shown. $\omega_{p1}=\omega_{pb}=24.2\pi T_c$, $\Gamma_1=\pi T_c$, $\Gamma_b=10\pi T_c$, $\epsilon_{\parallel}=4$. The normal-state reflectivities for $f=1$ and $f=\frac{2}{3}$ are shown as dotted curves. The dashed curves are for $\epsilon_{\perp}=\epsilon_{\parallel}=\epsilon_{BCS}$, i.e., for isotropic superconducting grains.

a Hagen-Rubens behavior develops with an infinite slope and an upward curvature.

The drop in $\mathcal{R}(\omega)$ at the absorption edge is sharper than the Mattis-Bardeen formula⁴⁴ would predict, because we are not in the dirty limit. The rather low reflectivity at $f=1$ and $\omega > 2\Delta$ is due to the fairly low plasma frequency^{18,33} $\omega_p=0.62$ eV, which we have chosen for most of our calculations. For $f < 1$, the reflectivity is further reduced in this frequency regime because $\Gamma_b=10\Gamma_1$. Note that $\mathcal{R}(\omega > 2\Delta, T \ll T_c)$ differs from $\mathcal{R}(\omega > 2\Delta, T > T_c)$ much less when $f < 1$, as observed.^{17,20}

If the background material has the same normal-state conductivity as the superconductor, reflectivities as shown in Fig. 6 are obtained. Also shown in Fig. 6 is the effect of an increase in the dc conductivities by a factor of 10 to $10(\text{m}\Omega \text{ cm})^{-1}$. In situations like these, the drop in $\mathcal{R}(\omega, T \ll T_c)$ at the absorption edge is rather small and, in view of experimental uncertainties, would be hard to discern.²³

Assigning a low conductivity to the background material by either increasing the scattering rate or reducing the plasma frequency gives low reflectivities for $\omega > 2\Delta$ (Fig. 7), as observed in ceramics.^{16,17,19,20} A reduction in $\mathcal{R}(\omega > 2\Delta, T \ll T_c)$ also results, if the platelike shape of the superconducting grains is taken into account.¹⁹ A low plasma frequency ω_{pb} is easily understood in terms of oxygen deficiency in the background material.

If one takes this a step further and assumes the background to be insulating, then the reflectivities shown in Fig. 8 are obtained. In contrast to Fig. 7 there is a sharp absorption edge but for large frequencies an insulating or poorly conducting background give very much the same reflectivities. Approaching the percolation threshold, the

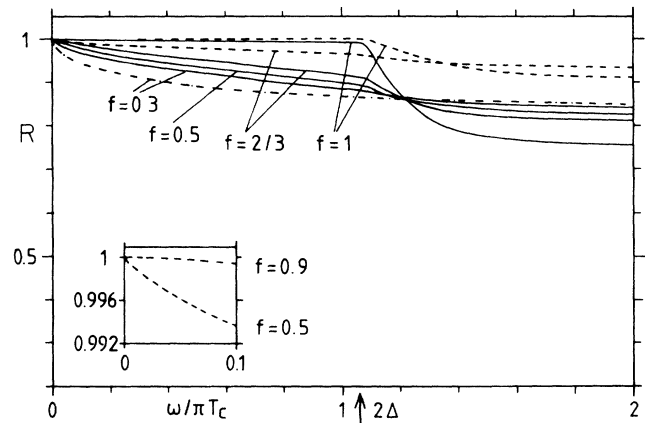


FIG. 6. EMA reflectivity for $0.5T_c$ for the case that the two components are equally good conductors in the normal state. Solid curves: $\sigma_{01}=\sigma_{0b}=23.2\pi T_c$, $\omega_{p1}=\omega_{pb}=24.2\pi T_c$, $\Gamma_1=\Gamma_b=\pi T_c$, $\epsilon_{\parallel}=4$. Also shown is the normal-state result (dash-dotted) for $f=0.3$. The dashed curves are obtained, if the dc conductivity is enhanced tenfold by increasing the plasma frequency and the scattering rate by factors of 5 and 2.5, respectively. In the inset the effect of the amount of normal conducting material on the zero-frequency slope is demonstrated for the latter parameter values.

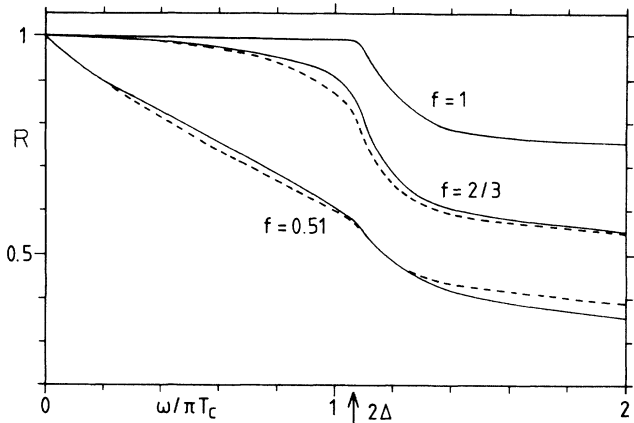


FIG. 7. EMA reflectivity for $0.5T_c$ for a poorly conducting background. The parameter values of the superconducting grains are $\omega_{p\perp} = 24.2\pi T_c$, $\Gamma_{\perp} = \pi T_c$, $\sigma_{0\perp} = 23.2\pi T_c$, $\epsilon_{\parallel} = 4$. Relative to $\sigma_{0\perp}$, the dc conductivity σ_{0b} is reduced by a factor of 100 in two ways: $\Gamma_b = 100\pi T_c$, $\omega_{pb} = \omega_{p\perp} = 24.2\pi T_c$ (dashed curves); $\omega_{pb} = 2.42\pi T_c$, $\Gamma_b = \Gamma_{\perp} = \pi T_c$ (solid curves).

absorption edge is shifted to lower frequencies. The shift is increased for frequencies above the percolation threshold if there is a finite permittivity along the c axis ($\epsilon_{\parallel} = 4$; dashed curves).

A downward shift of the absorption edge has been predicted previously by Sulewski *et al.*¹⁹ who applied the effective-medium approach to a one-component anisotropic medium. This corresponds to $f = 1$ in the present theory, where we find no such shift for $\epsilon_{\parallel} \leq 4$ (Fig. 8). Very large values of ϵ_{\parallel} are required [$\epsilon_{\parallel} = 35$ (Ref. 19)] to produce such a shift for $f = 1$. The shift can be increased further by choosing $g_{\parallel} \leq \frac{2}{3}$.¹⁹

In order to understand the nature of these new absorption edges, the calculations have to be extended to the plasma frequency, and, for simplicity, we shall assume that $\epsilon_{\parallel} = \epsilon_b = 1$. Our model now is equivalent to that of a mixture of *isotropic* superconducting grains and insulating ones.

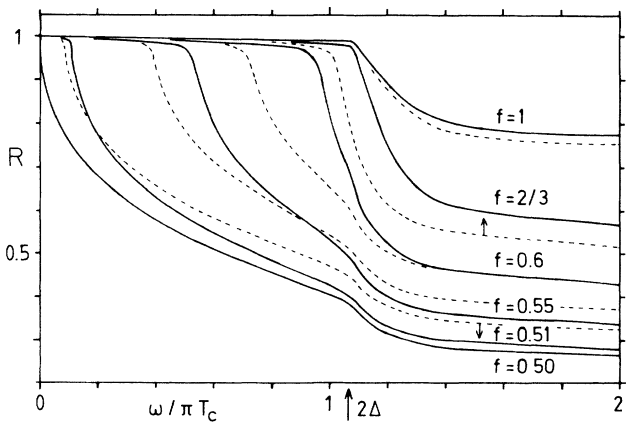


FIG. 8. EMA reflectivity at $T = 0.5T_c$ for uniaxial grains, insulating along the c axis, on an insulating background with $\epsilon_b = 1$, vs frequency. In this figure, the influence of the dielectric constant ϵ_{\parallel} along the c axis on the absorption edges is demonstrated. Solid curves: $\epsilon_{\parallel} = 1$, dashed curves: $\epsilon_{\parallel} = 4$. $\omega_{p\perp} = 24.2\pi T_c$, $\Gamma_{\perp} = \pi T_c$.

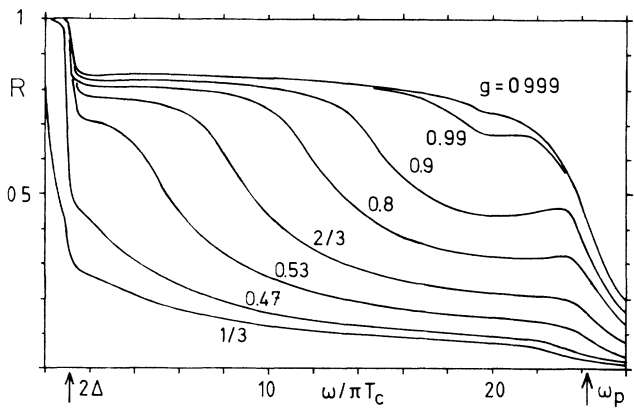


FIG. 9. EMA reflectivity of a composite of *isotropic*, superconducting grains on an insulating background. g denotes the volume fraction of the superconducting material. For $g \leq \frac{2}{3}$, this model is equivalent to the one with *uniaxial* grains having $\epsilon_{\parallel} = 1$ on a nonconducting background that also possesses $\epsilon_b = 1$, if $f = \frac{3}{2}g$ is inserted. The frequency scale has been extended up to the plasma frequency in order to show the occurrence of a void resonance at $\sqrt{\frac{2}{3}}\omega_p$ and its broadening as the amount of nonconducting material is increased. $\omega_p = 24.2\pi T_c$, $\Gamma = \pi T_c$, $T = 0.5T_c$.

We display the reflectivity of such a mixture in Fig. 9, where g denotes the volume fraction of the *isotropic* superconducting component. The relationship between f and g is $g = \frac{2}{3}f$, so the curves that are relevant for our *anisotropic* model are those between $g = \frac{2}{3}$ ($f = 1$) and the percolation threshold with $g = \frac{1}{3}$ ($f = \frac{1}{2}$).

If g is close to one, a *void resonance* develops at $\sqrt{\frac{2}{3}}\omega_p$ which broadens to what Stroud³⁰ calls an “impurity band”, if g is decreased. The little peak at the high-frequency edge diminishes and fades for $g = \frac{2}{3}$, the percolation limit for continuous *displacement currents*. The low-frequency edge moves towards lower frequencies and eventually reaches the region below the pair-breaking energy 2Δ and becomes visible in Fig. 8.

We see here a deficiency of the EMA: While uniaxial and two-component media are formally equivalent (for $g = \frac{2}{3}$), the notion of a void resonance makes no sense for a medium that is merely anisotropic but does not contain any physical voids. Since ceramic materials actually do contain voids it is conceivable that the low-energy gaps deduced from early experiments^{26,46} were, in fact, due to void resonances.

IV. CONCLUSIONS

Most aspects of the experimentally observed surface resistance $R_s(\omega, T)$ can be explained quantitatively using the effective-medium approach. Central to this interpretation of the measured $R_s(\omega, T)$ is the assumption that a fraction of each sample remains normal conducting, with a fairly high conductivity corresponding to $l \geq \xi_0$. If the Mattis-Bardeen formula,⁴⁴ valid for $l \rightarrow 0$, is used, the EMA fails to account for the observed residual resistance.⁴⁷ The amount of normal metal, whose presence

one has to postulate, is reduced to more reasonable values through the anisotropic conductivity in the grains as well as their platelike shape.

The presence of a good normal metal in the superconducting state of most high- T_c materials could also be inferred from tunneling data obtained on $\text{YBa}_2\text{Cu}_3\text{O}_{7-\delta}$ -barrier-Pb junctions that show a strong signal due to tunneling from superconducting lead into a normal metal,⁴⁸ and from specific-heat measurements on $\text{YBa}_2\text{Cu}_3\text{O}_{7-\delta}$ in which large linear terms have been observed.⁴⁹ Specific-heat measurements as well as the R_s data show that the size of the normal component depends on preparation technique, as one would expect.

Inconsistent with this picture, however, is the absence of a linear term in the low-temperature specific heat of the Bi-Ca-Sr-Cu system⁴⁹ while measurements of the surface resistance on these compounds¹² showed residual resistances comparable to those observed in $\text{YBa}_2\text{Cu}_3\text{O}_{7-\delta}$. An independent identification and quantification of this "normal component" would, therefore, be most desirable.

As we have stated earlier,¹³ nodes in the energy gap do not provide a compelling alternative explanation of the observed residual resistance. Using permittivities for such unconventional states we still have to invoke the presence of some normal metal to obtain qualitatively similar fits to the data. There is a difference at low temperatures, however, where unconventional states do not lead to a saturation of R_s . While this is in qualitative agreement with some experiments (e.g., Refs. 2, 4, 8, and 9), the calculated temperature dependence is close to quadratic and not linear as observed in most cases.^{8,9}

The presence of some normal conducting component also helps to understand some features of the observed in-

frared reflectivity, as noted before.^{16,17} If an insulating material is also present, a shift of the absorption edge to lower frequencies due to a void resonance³⁰ can occur. There seems to be no way in which an increased energy gap can result from granularity.

While the present theory allows us to estimate the effect of some defects on the electromagnetic response of anisotropic superconductors, it is far from providing a complete picture. For example, polishing the surface reduces the surface resistance.⁴ While it is conceivable that such a surface treatment changes the average composition of the sample within the penetration depth, we tend to believe that it is the change in surface roughness that is ultimately responsible for lowering R_s . Our theory in its present form is only applicable to plane interfaces. Furthermore, while we have drawn attention to the importance of keeping finite mean free paths we have not been able to include inelastic scattering that might be responsible for the temperature dependence of the residual surface resistance^{2,8,9} as well as that of the infrared reflectivity.^{18,23} It seems, therefore, that we still have a long way to go before measurements of the electromagnetic response will actually shed some light on the nature of the superconducting state in the new oxide superconductors.

ACKNOWLEDGMENTS

We would like to thank G. Grüner for providing us with experimental data. Valuable and motivating discussions we had with H. Piel, K. F. Renk, K. Baberschke, and M. Hein have been highly appreciated. One of the authors (D. W.) gratefully acknowledges a grant from the Studienstiftung des Deutschen Volkes.

¹A. M. Awasthi, J. P. Carini, B. Alavi, and G. Grüner, *Solid State Commun.* **67**, 373 (1988).

²H. Piel, M. Hein, N. Klein, U. Klein, A. Michalke, G. Müller, and L. Ponto, *Physica C* **153-155**, 1604 (1988).

³J. P. Carini and G. Grüner, *Phys. Scr.* **T25**, 72 (1989).

⁴M. Hein, G. Müller, H. Piel, U. Klein, and M. Peiniger, *J. Less-Common Met.* **151**, 71 (1989).

⁵N. Klein, G. Müller, H. Piel, B. Roas, L. Schultz, U. Klein, and M. Peiniger, *Appl. Phys. Lett.* **54**, 757 (1989).

⁶S. Sridhar, C. A. Shiffman, and H. Hamdek, *Phys. Rev. B* **36**, 201 (1987).

⁷W. L. Kennedy and S. Sridhar, *Solid State Commun.* **68**, 71 (1988).

⁸J. P. Carini, A. M. Awasthi, W. Beyermann, G. Grüner, T. Hylton, K. Char, M. R. Beasley, and A. Kapitulnik, *Phys. Rev. B* **37**, 9726 (1988).

⁹L. Drabeck, J. P. Carini, G. Grüner, T. Hylton, K. Char, and M. R. Beasley, *Phys. Rev. B* **39**, 785 (1989).

¹⁰N. Klein, G. Müller, S. Orbach, H. Piel, H. Chaloupka, B. Roas, L. Schultz, U. Klein, and M. Peiniger, *Physica C* **162-164**, 1549 (1989).

¹¹D. W. Cooke, E. R. Gray, H. H. S. Javadi, R. J. Houlton, B. Rusbak, E. A. Meyer, P. N. Arendt, N. Klein, G. Müller, S. Orbach, H. Piel, L. Drabeck, G. Grüner, J. Y. Josefovich, D. B. Rensch, and F. Krajenbrink, *Solid State Commun.* **73**, 297

(1990); *Physica C* **162-164**, 1537 (1989).

¹²C. L. Bohn, J. R. Delayen, U. Balachandran, and M. T. Lanagan, *Appl. Phys. Lett.* **55**, 304 (1989).

¹³R. A. Klemm, K. Scharnberg, D. Walker, and C. T. Rieck, *Z. Phys. B* **72**, 139 (1988).

¹⁴D. L. Rubin, K. Green, J. Gruschus, J. Kirchgessner, D. Moffat, H. Padamsee, J. Sears, Q. S. Shu, L. F. Schneemeyer, and J. V. Waszczak, *Phys. Rev. B* **38**, 6538 (1988).

¹⁵J. Garner and D. Stroud, *Phys. Rev. B* **28**, 2447 (1983).

¹⁶G. A. Thomas, H. K. Ng, A. J. Millis, R. N. Bhatt, R. J. Cava, E. A. Rietman, D. W. Johnston, Jr., G. P. Espinosa, and J. M. Vandenberg, *Phys. Rev. B* **36**, 846 (1987).

¹⁷A. Wittlin, L. Genzel, M. Cardona, M. Bauer, W. König, E. García, M. Barahona, and M. V. Cabañas, *Phys. Rev. B* **37**, 652 (1988).

¹⁸G. A. Thomas, J. Orenstein, D. H. Rapkine, M. Capizzi, A. J. Millis, R. N. Bhatt, L. F. Schneemeyer, and J. V. Waszczak, *Phys. Rev. Lett.* **61**, 1313 (1988).

¹⁹P. E. Sulewski, T. W. Noh, J. T. McWhirter, and A. J. Sievers, *Phys. Rev. B* **36**, 5735 (1987).

²⁰T. W. Noh, P. E. Sulewski, and A. J. Sievers, *Phys. Rev. B* **36**, 8866 (1987).

²¹Z. Schlesinger, R. T. Collins, D. L. Kaiser, and F. Holtzberg, *Phys. Rev. Lett.* **59**, 1958 (1987).

²²T. Timusk, D. A. Bonn, J. E. Greedan, C. V. Stager, J. D.

- Garrett, A. H. O'Reilly, M. Reedyk, K. Kamarás, C. D. Porter, S. L. Herr, and D. B. Tanner, *Physica C* **153-155**, 1744 (1988).
- ²³T. Timusk and D. B. Tanner, in *Physical Properties of High Temperature Superconductors I*, edited by D. M. Ginsberg (World Scientific, Singapore, 1989), p. 339.
- ²⁴W. Ose, P. E. Obermayer, H. H. Otto, T. Zetterer, H. Langfellner, J. Keller, and K. F. Renk, *Z. Phys. B* **70**, 307 (1988); W. Ose, P. E. Obermayer, H. H. Otto, T. Zetterer, H. Langfellner, H. Tasler, J. Keller, and K. F. Renk, *Physica C* **153-155**, 639 (1988).
- ²⁵J. Schützmann, W. Ose, J. Keller, K. F. Renk, B. Roas, L. Schultz, and G. Saemann-Ischenko, *Europhys. Lett.* **8**, 679 (1989).
- ²⁶R. T. Collins, Z. Schlesinger, R. H. Koch, R. B. Laibowitz, T. S. Plaskett, P. Freitas, W. J. Gallagher, R. L. Sandstrom, and T. R. Dinger, *Phys. Rev. Lett.* **59**, 704 (1987).
- ²⁷P. Chaudhari, R. T. Collins, P. Freitas, R. J. Gambino, J. R. Kirtley, R. H. Koch, R. B. Laibowitz, F. K. LeGoues, T. R. McGuire, T. Penney, Z. Schlesinger, A. P. Segmüller, S. Foner, and E. J. McNiff, Jr., *Phys. Rev. B* **36**, 8903 (1987).
- ²⁸G. L. Carr, S. Perkowitz, and D. B. Tanner, in *Infrared and Millimetre Waves*, edited by K. J. Button (Academic, London 1985), Vol. 13, p. 171.
- ²⁹D. M. Wood and N. W. Ashcroft, *Philos. Mag.* **35**, 269 (1977).
- ³⁰D. Stroud, *Phys. Rev. B* **19**, 1783 (1979); **12**, 3368 (1975).
- ³¹R. J. Elliott, J. A. Krumhansl, and P. L. Leath, *Rev. Mod. Phys.* **46**, 535 (1974).
- ³²J. Orenstein and D. H. Rapkine, *Phys. Rev. Lett.* **60**, 968 (1988).
- ³³W. Markowitsch, W. Lang, N. S. Sariciftci, and G. Leising, *Solid State Commun.* **69**, 363 (1989).
- ³⁴G. L. Doll, J. Steinbek, G. Dresselhaus, M. S. Dresselhaus, A. J. Strauss, and H. J. Zeiger, *Phys. Rev. B* **36**, 8884 (1987).
- ³⁵J. R. Clem, *Physica C* **153-155**, 50 (1988).
- ³⁶C. Jeffries, Q. H. Lam, L. C. Bourne, and A. Zettl, *Phys. Rev. B* **37**, 9840 (1988).
- ³⁷T.-K. Xia and D. Stroud, *Phys. Rev. B* **37**, 118 (1988); (unpublished).
- ³⁸M. Tinkham and C. J. Lobb, in *Solid State Physics*, edited by H. Ehrenreich and D. Turnbull (Academic, New York, 1989), Vol. 42, p. 91.
- ³⁹L. D. Landau and E. M. Lifshitz, *Electrodynamics of Continuous Media, Course of Theoretical Physics* (Pergamon, Oxford, 1960), Vol. 8.
- ⁴⁰M. Tinkham, *Introduction to Superconductivity* (Krieger, Malabar, 1985).
- ⁴¹R. L. Greene, L. Krusin-Elbaum, and A. P. Malozemoff, *Phys. Rev. Lett.* **62**, 2886 (1989); A. F. Hebard, A. F. Fiory, and D. R. Harshman, *ibid.* **62**, 2885 (1989).
- ⁴²S. M. Anlage, H. Sze, H. J. Snortland, S. Tahara, B. Langley, C.-B. Eom, M. R. Beasley, and R. Taber, *Appl. Phys. Lett.* **54**, 2710 (1989).
- ⁴³K. Scharnberg, *J. Low Temp. Phys.* **30**, 229 (1978).
- ⁴⁴D. Mattis and J. Bardeen, *Phys. Rev.* **111**, 412 (1958).
- ⁴⁵T. L. Hylton and M. R. Beasley, *Phys. Rev. B* **39**, 9042 (1988).
- ⁴⁶S. Sugai, S. Uchida, H. Takagi, K. Kitazawa, S. Tanaka, M. Sato, and S. Hosoya, *Physica B* **148**, 282 (1987).
- ⁴⁷L. Genzel, A. Wittlin, M. Bauer, M. Cardona, E. Schönherr, and A. Simon, *Phys. Rev. B* **40**, 2170 (1989).
- ⁴⁸J. Geerk, X. X. Xi, and G. Linker, *Z. Phys. B* **73**, 329 (1988).
- ⁴⁹R. A. Fisher, S. Kim, S. E. Lacy, N. E. Phillips, D. E. Morris, A. G. Markelz, J. Y. T. Wei, and D. S. Ginley, *Phys. Rev. B* **38**, 11 942 (1988).